Electronic Supplementary Material (ESI) for MedChemComm.
This journal is © The Royal Society of Chemistry 2018

Electronic Supporting Information Materials

Platinum(II) complexes with rutaecarpine and tryptanthrin derivatives induce apoptosis by inhibiting telomerase activity and disrupting mitochondrial function

Qi-Pin Qin [a,d,1], Bi-Qun Zou [a,c,d, 1], Fei-Long Hu [b], Guo-Bao Huang [a], Shu-Long Wang [a,d], Yun-Qiong Gu [a,d] and Ming-Xiong Tan [a,*]

Table S1. Crystal data and structure refinement details for **Rut-Pt**.

Empirical formula	$C_{20}H_{18}Cl_2N_3O_2PtS$
Formula weight	630.42
Temperature/K	296.15
Crystal system	monoclinic
Space group	$P2_1/n$
a/Å	11.4250(2)
b/Å	15.9927(3)
c/Å	11.9390(2)
α/°	90.00
β/°	105.0510(10)
γ/°	90.00
Volume/Å^3	2106.62(6)
Z	4
ρ_{calc}mg/mm^3	1.988
m/mm^{-1}	7.036
F(000)	1212.0
2Θ range for data collection	4.36 to 50°
Index ranges	$-13 \le h \le 13$, $-19 \le k \le 17$, $-14 \le l \le 14$
Reflections collected	15089
Independent reflections	3717[R(int) = 0.0292]
Data/restraints/parameters	3717/0/264
Goodness-of-fit on F^2	1.080
Final R indexes [I>=2σ (I)]	R_1 = 0.1004, wR_2 = 0.2293
Final R indexes [all data]	R_1 = 0.1098, wR_2 = 0.2353
Largest diff. peak/hole / e Å^{-3}	11.49/-4.30

[a] $R_1 = \Sigma \, ||F_o| - |F_c|| / \Sigma |F_o|$; [b] $wR_2 = [\Sigma w(F_o^2 - F_c^2)^2 / \Sigma w(F_o^2)^2]^{1/2}$.

Table S2. Selected bond lengths (Å) for **Rut-Pt**.

Atom	Atom	Length/Å	Atom	Atom	Length/Å
C1	C2	1.39(2)	C11	C21	1.52(2)
C1	C6	1.38(2)	C12	C21	1.46(2)
C1	N1	1.418(18)	C13	C14	1.43(2)
C2	C3	1.39(2)	C13	C18	1.42(2)
C3	C4	1.37(3)	C14	C15	1.37(2)
C4	C5	1.36(2)	C14	N2	1.384(18)
C5	C6	1.41(2)	C15	C16	1.36(2)
C6	C7	1.47(2)	C16	C17	1.38(2)
C7	N3	1.45(2)	C17	C18	1.35(2)
C7	O1	1.189(18)	C19	S1	1.737(18)
N3	C9	1.343(18)	C20	S1	1.78(2)
N3	C12	1.498(19)	Cl1	Pt1	2.288(4)
C9	C10	1.45(2)	Cl2	Pt1	2.344(4)
C9	N1	1.319(18)	N1	Pt1	2.066(12)
C10	C11	1.368(19)	O2	S1	1.402(12)
C10	N2	1.399(18)	Pt1	S1	2.200(4)
C11	C13	1.41(2)			

Table S3. Selected bond angles (°) for **Rut-Pt**.

Atom	Atom	Atom	Angle/°	Atom	Atom	Atom	Angle/°
C2	C1	N1	119.6(13)	C11	C13	C18	135.1(14)
C6	C1	C2	119.7(14)	C18	C13	C14	117.8(14)
C6	C1	N1	120.6(13)	C15	C14	C13	121.8(14)
C3	C2	C1	119.1(16)	C15	C14	N2	130.2(14)
C4	C3	C2	120.7(16)	N2	C14	C13	108.0(13)
C5	C4	C3	120.9(16)	C16	C15	C14	117.6(15)
C4	C5	C6	119.2(16)	C15	C16	C17	122.7(16)
C1	C6	C5	120.4(15)	C18	C17	C16	120.9(16)
C1	C6	C7	121.3(14)	C17	C18	C13	119.1(16)
C5	C6	C7	118.3(14)	C1	N1	Pt1	116.6(9)
N3	C7	C6	112.2(12)	C9	N1	C1	119.2(12)
O1	C7	C6	126.1(15)	C9	N1	Pt1	123.2(9)
O1	C7	N3	121.4(15)	C14	N2	C10	107.2(12)
C7	N3	C12	114.1(12)	C12	C21	C11	109.2(12)
C9	N3	C7	123.9(13)	Cl1	Pt1	Cl2	172.21(16)
C9	N3	C12	122.0(13)	N1	Pt1	Cl1	89.2(3)
N3	C9	C10	114.2(13)	N1	Pt1	Cl2	86.1(3)
N1	C9	N3	122.6(13)	N1	Pt1	S1	174.5(3)
N1	C9	C10	123.2(12)	S1	Pt1	Cl1	94.72(16)
C11	C10	C9	122.7(13)	S1	Pt1	Cl2	90.34(15)
C11	C10	N2	110.2(12)	C19	S1	C20	100.8(12)
N2	C10	C9	126.5(12)	C19	S1	Pt1	109.3(7)
C10	C11	C13	107.4(13)	C20	S1	Pt1	108.5(8)
C10	C11	C21	119.3(13)	O2	S1	C19	113.0(10)
C13	C11	C21	133.2(13)	O2	S1	C20	111.7(13)
C21	C12	N3	112.0(12)	O2	S1	Pt1	112.8(6)
C11	C13	C14	107.1(12)				

Table S4. Crystal data and structure refinement details for **Try-Pt**.

Empirical formula	$C_{17}H_{14}Cl_2N_2O_3PtS$
Formula weight	592.35
Temperature/K	293(2)
Crystal system	triclinic
Space group	P-1
a/Å	8.51960(10)
b/Å	9.9538(2)
c/Å	10.8961(2)
α/°	95.0330(10)
β/°	90.1660(10)
γ/°	98.3380(10)
Volume/Å^3	910.61(3)
Z	2
ρ_{calc}mg/mm^3	2.160
m/mm^{-1}	8.133
F(000)	564.0
2Θ range for data collection	3.76 to 55.4°
Index ranges	$-10 \leq h \leq 11$, $-13 \leq k \leq 12$, $-13 \leq l \leq 14$
Reflections collected	14970
Independent reflections	4204[R(int) = 0.0225]
Data/restraints/parameters	4204/0/237
Goodness-of-fit on F^2	1.099
Final R indexes [I>=2σ (I)]	R_1 = 0.0503, wR_2 = 0.1256
Final R indexes [all data]	R_1 = 0.0544, wR_2 = 0.1279
Largest diff. peak/hole / e Å^{-3}	7.82/-1.20

[a] $R_1 = \Sigma \, ||F_o| - |F_c|| / \Sigma |F_o|$; [b] $wR_2 = [\Sigma w(F_o^2 - F_c^2)^2 / \Sigma w(F_o^2)^2]^{½}$.

Table S5. Selected bond lengths (Å) for **Try-Pt**.

Atom	Atom	Length/Å	Atom	Atom	Length/Å
C1	C2	1.402(15)	C10	C11	1.472(13)
C1	C6	1.392(13)	C10	C12	1.398(13)
C2	C3	1.352(18)	C11	N2	1.382(12)
C3	C4	1.388(16)	C11	O2	1.222(11)
C4	C5	1.384(13)	C12	C13	1.374(16)
C5	C6	1.397(13)	C13	C14	1.382(17)
C5	N2	1.442(11)	C14	C15	1.374(14)
C6	C7	1.445(12)	C16	S1	1.774(10)
C7	C8	1.536(12)	O3	S1	1.475(7)
C7	O1	1.205(11)	C18	S1	1.756(10)
C8	N1	1.283(11)	Cl1	Pt1	2.320(2)
C8	N2	1.375(10)	Cl2	Pt1	2.302(3)
C9	C10	1.395(13)	S1	Pt1	2.201(2)
C9	C15	1.395(13)	N1	Pt1	2.082(7)
C9	N1	1.411(11)			

Table S6. Selected bond angles (°) for **Try-Pt**.

Atom	Atom	Atom	Angle/°	Atom	Atom	Atom	Angle/°
C6	C1	C2	117.0(10)	O2	C11	N2	121.6(9)
C3	C2	C1	120.6(10)	C13	C12	C10	119.2(10)
C2	C3	C4	123.8(10)	C12	C13	C14	120.7(9)
C5	C4	C3	116.1(10)	C15	C14	C13	121.2(10)
C4	C5	C6	121.4(9)	C14	C15	C9	118.9(9)
C4	C5	N2	129.7(9)	C16	S1	Pt1	110.6(4)
C6	C5	N2	108.9(7)	O3	S1	C16	108.5(6)
C1	C6	C5	121.1(9)	O3	S1	C18	110.7(5)
C1	C6	C7	129.1(9)	O3	S1	Pt1	116.9(4)
C5	C6	C7	109.7(8)	C18	S1	C16	103.2(7)
C6	C7	C8	104.1(7)	C18	S1	Pt1	106.0(4)
O1	C7	C6	130.5(9)	C8	N1	C9	118.4(7)
O1	C7	C8	125.3(8)	C8	N1	Pt1	120.3(6)
N1	C8	C7	127.9(7)	C9	N1	Pt1	121.2(6)
N1	C8	N2	124.2(8)	C8	N2	C5	109.4(7)
N2	C8	C7	107.7(7)	C8	N2	C11	123.3(7)
C10	C9	N1	119.9(8)	C11	N2	C5	127.2(7)
C15	C9	C10	120.2(8)	Cl2	Pt1	Cl1	174.54(9)
C15	C9	N1	119.8(8)	S1	Pt1	Cl1	90.97(9)
C9	C10	C11	121.0(8)	S1	Pt1	Cl2	93.78(9)
C9	C10	C12	119.9(9)	N1	Pt1	Cl1	88.8(2)
C12	C10	C11	119.2(9)	N1	Pt1	Cl2	86.5(2)
N2	C11	C10	113.0(7)	N1	Pt1	S1	178.9(2)
O2	C11	C10	125.4(9)				

Table S7. Crystal data and structure refinement details for **ITry-Pt**.

Empirical formula	$C_{17}H_{13}Cl_2IN_2O_3PtS$
Formula weight	718.24
Temperature/K	293(2)
Crystal system	monoclinic
Space group	$P2_1/c$
a/Å	8.59400(10)
b/Å	11.5135(2)
c/Å	21.0202(3)
α/°	90.00
β/°	108.1880(10)
γ/°	90.00
Volume/Å^3	1975.97(5)
Z	4
ρ_{calc}mg/mm^3	2.414
m/mm^{-1}	9.061
F(000)	1336.0
Crystal size/mm^3	? × ? × ?
2Θ range for data collection	4.08 to 54.9°
Index ranges	$-9 \le h \le 11$, $-14 \le k \le 13$, $-26 \le l \le 27$
Reflections collected	16917
Independent reflections	4492[R(int) = 0.0378]
Data/restraints/parameters	4492/0/246
Goodness-of-fit on F^2	1.044
Final R indexes [I>=2σ (I)]	R_1 = 0.0531, wR_2 = 0.1591
Final R indexes [all data]	R_1 = 0.0764, wR_2 = 0.1733
Largest diff. peak/hole / e Å^{-3}	4.03/-3.13

[a] $R_1 = \Sigma \, ||F_o| - |F_c|| / \Sigma |F_o|$; [b] $wR_2 = [\Sigma w(F_o^2 - F_c^2)^2 / \Sigma w(F_o^2)^2]^{½}$.

Table S8. Selected bond lengths (Å) for **ITry-Pt**.

Atom	Atom	Length/Å	Atom	Atom	Length/Å
Pt1	Cl1	2.302(3)	C1	C2	1.370(16)
Pt1	Cl2	2.314(3)	C1	C6	1.393(15)
Pt1	S1	2.203(3)	C2	C3	1.381(17)
Pt1	N1	2.060(9)	C3	C4	1.41(2)
I1	C14	2.097(13)	C4	C5	1.34(2)
S1	O1	1.444(8)	C5	C6	1.365(16)
S1	C16	1.782(12)	C6	C7	1.477(17)
S1	C17	1.768(12)	C8	C9	1.492(15)
O2	C7	1.204(14)	C9	C10	1.488(15)
O3	C9	1.190(12)	C10	C11	1.363(16)
N1	C1	1.430(13)	C10	C15	1.387(16)
N1	C8	1.311(14)	C11	C12	1.391(15)
N2	C7	1.384(13)	C12	C13	1.384(19)
N2	C8	1.383(12)	C13	C14	1.391(19)
N2	C11	1.422(15)	C14	C15	1.372(17)

Table S9. Selected bond angles (°) for **ITry-Pt**.

Atom	Atom	Atom	Angle/°	Atom	Atom	Atom	Angle/°
Cl1	Pt1	Cl2	90.96(12)	C1	C6	C7	121.1(10)
S1	Pt1	Cl1	91.03(11)	C5	C6	C1	119.6(12)
S1	Pt1	Cl2	177.92(11)	C5	C6	C7	119.4(11)
N1	Pt1	Cl1	177.6(3)	O2	C7	N2	121.8(11)
N1	Pt1	Cl2	87.7(3)	O2	C7	C6	125.4(10)
N1	Pt1	S1	90.3(3)	N2	C7	C6	112.8(9)
O1	S1	Pt1	114.2(4)	N1	C8	N2	124.1(10)
O1	S1	C16	109.7(6)	N1	C8	C9	127.0(10)
O1	S1	C17	108.1(6)	N2	C8	C9	108.9(9)
C16	S1	Pt1	107.6(5)	O3	C9	C8	127.5(11)
C17	S1	Pt1	114.4(5)	O3	C9	C10	129.2(11)
C17	S1	C16	101.9(7)	C10	C9	C8	103.3(9)
C1	N1	Pt1	121.9(7)	C11	C10	C9	108.8(10)
C8	N1	Pt1	121.2(7)	C11	C10	C15	121.9(11)
C8	N1	C1	116.8(9)	C15	C10	C9	129.3(11)
C7	N2	C11	127.4(9)	C10	C11	N2	110.4(9)
C8	N2	C7	124.1(9)	C10	C11	C12	121.6(12)
C8	N2	C11	108.4(9)	C12	C11	N2	127.9(11)
C2	C1	N1	118.7(10)	C13	C12	C11	116.2(12)
C2	C1	C6	120.3(10)	C12	C13	C14	122.2(12)
C6	C1	N1	121.0(10)	C13	C14	I1	119.3(9)
C1	C2	C3	119.8(12)	C15	C14	I1	120.1(10)
C2	C3	C4	118.8(13)	C15	C14	C13	120.5(12)
C5	C4	C3	120.6(12)	C14	C15	C10	117.6(12)
C4	C5	C6	120.9(12)				

Table S10. Crystal data and structure refinement details for **BrTry-Pt**.

Empirical formula	$C_{18}H_{17}BrCl_2N_2O_4PtS$
Formula weight	703.30
Temperature/K	296.15
Crystal system	monoclinic
Space group	C2/c
a/Å	23.8724(5)
b/Å	7.9160(2)
c/Å	23.4616(5)
α/°	90.00
β/°	106.9840(10)
γ/°	90.00
Volume/Å^3	4240.26(17)
Z	8
ρ_{calc}mg/mm^3	2.203
m/mm^{-1}	8.881
F(000)	2672.0
Crystal size/mm^3	? × ? × ?
2Θ range for data collection	3.56 to 55.12°
Index ranges	$-30 \le h \le 29$, $-10 \le k \le 10$, $-29 \le l \le 30$
Reflections collected	18016
Independent reflections	4890[R(int) = 0.0367]
Data/restraints/parameters	4890/0/266
Goodness-of-fit on F^2	1.058
Final R indexes [I>=2σ (I)]	$R_1 = 0.0356$, $wR_2 = 0.0813$
Final R indexes [all data]	$R_1 = 0.0540$, $wR_2 = 0.0877$
Largest diff. peak/hole / e Å^{-3}	1.36/-0.95

[a] $R_1 = \Sigma\, ||F_o| - |F_c||/\Sigma|F_o|$; [b] $wR_2 = [\Sigma w(F_o^2 - F_c^2)^2/\Sigma w(F_o^2)^2]^{½}$.

Table S11. Selected bond lengths (Å) for **BrTry-Pt**.

Atom	Atom	Length/Å	Atom	Atom	Length/Å
Br1	C3	1.895(6)	C10	C11	1.399(8)
C1	C2	1.375(9)	C10	C15	1.401(9)
C1	C6	1.387(8)	C11	C12	1.403(8)
C1	C8	1.475(8)	C11	N2	1.399(7)
C2	C3	1.376(8)	C12	C13	1.358(9)
C3	C4	1.384(9)	C13	C14	1.389(10)
C4	C5	1.391(9)	C14	C15	1.362(10)
C5	C6	1.385(8)	C16	S1	1.786(7)
C6	N1	1.428(8)	C17	S1	1.763(7)
C7	C8	1.516(8)	Cl1	Pt1	2.2925(17)
C7	N1	1.382(7)	Cl2	Pt1	2.2946(17)
C7	N2	1.282(7)	N2	Pt1	2.094(5)
C8	O1	1.200(7)	O3	S1	1.460(4)
C9	C10	1.449(9)	Pt1	S1	2.2069(15)
C9	N1	1.397(7)	O4	C19	1.386(9)
C9	O2	1.220(7)			

Table S12. Selected bond angles (°) for **BrTry-Pt**.

Atom	Atom	Atom	Angle/°	Atom	Atom	Atom	Angle/°
C2	C1	C6	120.8(6)	N2	C11	C10	120.3(5)
C2	C1	C8	130.9(6)	N2	C11	C12	120.4(5)
C6	C1	C8	108.3(5)	C13	C12	C11	120.4(6)
C1	C2	C3	118.1(6)	C12	C13	C14	120.4(7)
C2	C3	Br1	120.1(5)	C15	C14	C13	120.3(6)
C2	C3	C4	121.4(6)	C14	C15	C10	120.5(6)
C4	C3	Br1	118.5(5)	C7	N1	C6	109.7(5)
C3	C4	C5	121.0(6)	C7	N1	C9	122.7(5)
C6	C5	C4	117.1(6)	C9	N1	C6	127.6(5)
C1	C6	N1	109.9(5)	C7	N2	C11	118.0(5)
C5	C6	C1	121.6(6)	C7	N2	Pt1	119.6(4)
C5	C6	N1	128.5(5)	C11	N2	Pt1	122.2(4)
N1	C7	C8	107.4(5)	Cl1	Pt1	Cl2	175.98(7)
N2	C7	C8	128.1(5)	N2	Pt1	Cl1	88.29(14)
N2	C7	N1	124.5(5)	N2	Pt1	Cl2	88.78(14)
C1	C8	C7	104.6(5)	N2	Pt1	S1	175.82(13)
O1	C8	C1	130.1(6)	S1	Pt1	Cl1	88.08(6)
O1	C8	C7	125.3(6)	S1	Pt1	Cl2	94.95(6)
N1	C9	C10	112.6(5)	C16	S1	Pt1	113.0(3)
O2	C9	C10	127.5(6)	C17	S1	C16	100.7(4)
O2	C9	N1	119.9(6)	C17	S1	Pt1	107.5(3)
C11	C10	C9	121.6(6)	O3	S1	C16	108.6(3)
C11	C10	C15	118.9(6)	O3	S1	C17	108.4(3)
C15	C10	C9	119.4(6)	O3	S1	Pt1	117.27(19)
C10	C11	C12	119.3(6)				

Table S13. Inhibitory rates (%) of cisplatin, Rut, Try, ITry, BrTry, *cis*-Pt(DMSO)$_2$Cl$_2$, **Rut-Pt**, **Try-Pt**, **ITry-Pt** and **BrTry-Pt** toward on the selected six human cells for 48 h.

Compounds	T-24	A549	Hep-G2	SK-OV-3	HeLa	HL-7702
Rut [a]	23.15±0.43	20.13±0.88	25.09±1.49	20.36±0.49	24.01±0.25	28.06±1.85
Rut-Pt [a]	38.09±0.51	23.52±1.59	21.34±0.65	40.35±2.03	26.88±2.59	31.25±0.45
Try [a]	20.19±1.78	22.26±1.06	30.25±0.59	32.52±0.81	28.56±0.65	34.03±1.27
Try-Pt [a]	40.12±1.63	26.66±2.31	29.49±1.90	42.63±0.39	29.68±0.76	33.05±0.62
ITry [a]	34.25±0.92	27.98±1.49	30.31±0.75	33.87±1.01	29.45±1.67	32.87±1.20
ITry-Pt [a]	57.03±1.03	29.24±1.16	33.51±0.42	56.71±0.32	35.09±0.47	33.98±0.66
BrTry [a]	60.26±0.91	31.06±1.25	35.81±0.57	36.88±2.07	30.03±2.33	39.54±0.55
BrTry-Pt [a]	84.34±0.29	45.26±0.80	44.92±0.81	69.96±0.48	39.59±1.99	31.25±1.23
cis-Pt(DMSO)$_2$Cl$_2$ [b]	23.15±0.94	30.25±0.96	21.03±1.72	29.78±2.77	23.64±2.13	20.16±0.85
Cisplatin [a,c]	60.12±1.19	60.58±2.01	57.45±0.61	60.88±1.55	69.45±1.06	58.11±1.39

Results represent mean ± SD of at least six independent experiments. SD represents the standard deviation. [a] The concentration is 20.0 μM. [b] The concentration is 100.0 μM. [c] Cisplatin was dissolved at a concentration of 1.0 mM in 0.154 M NaCl.

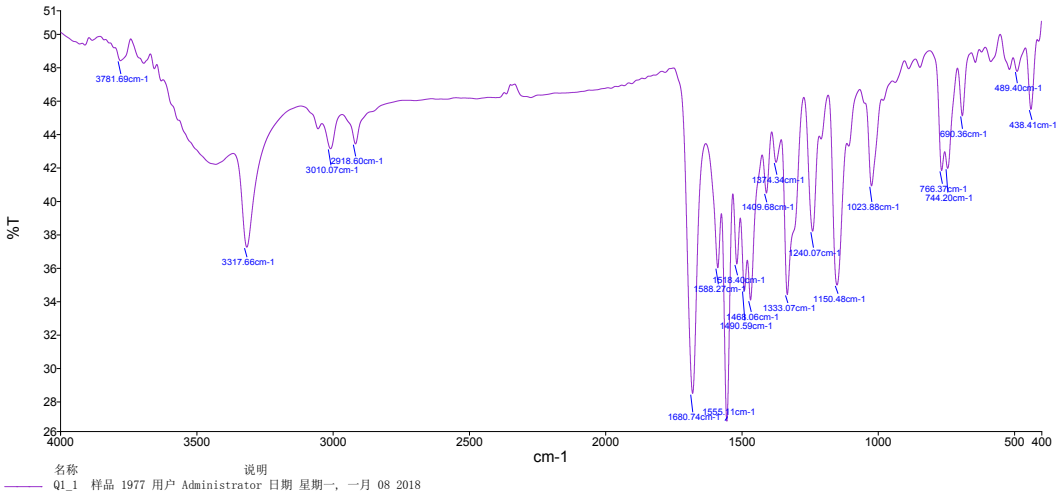

Fig. S1. IR (KBr) spectra of **Rut-Pt**

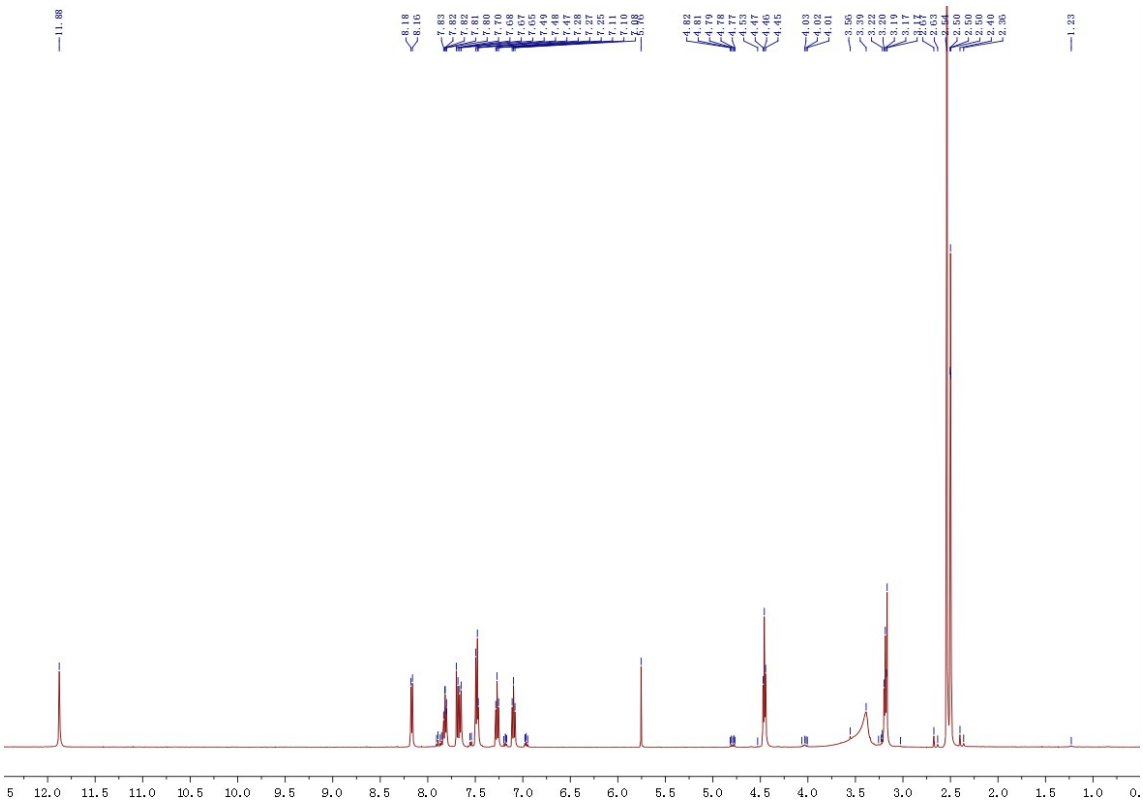

Fig. S2. ^{1}H NMR (500MHz, DMSO-d_6) for **Rut-Pt**

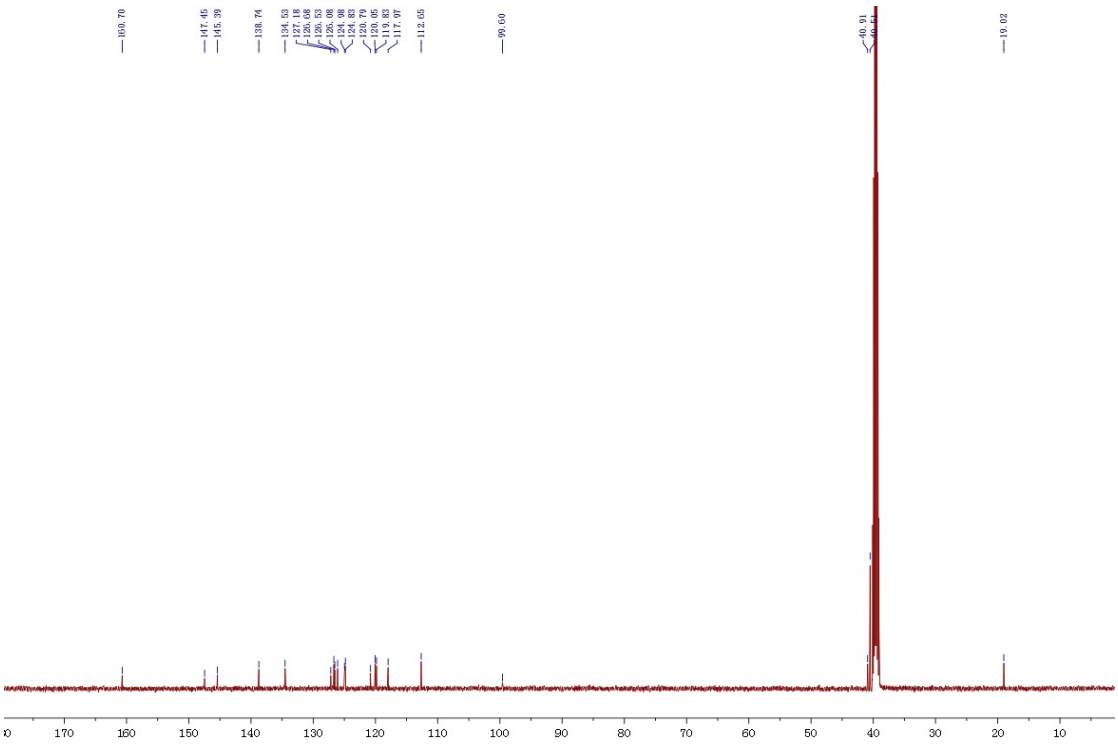

Fig. S3. ^{13}C NMR (126MHz, DMSO-d_6) for **Rut-Pt**

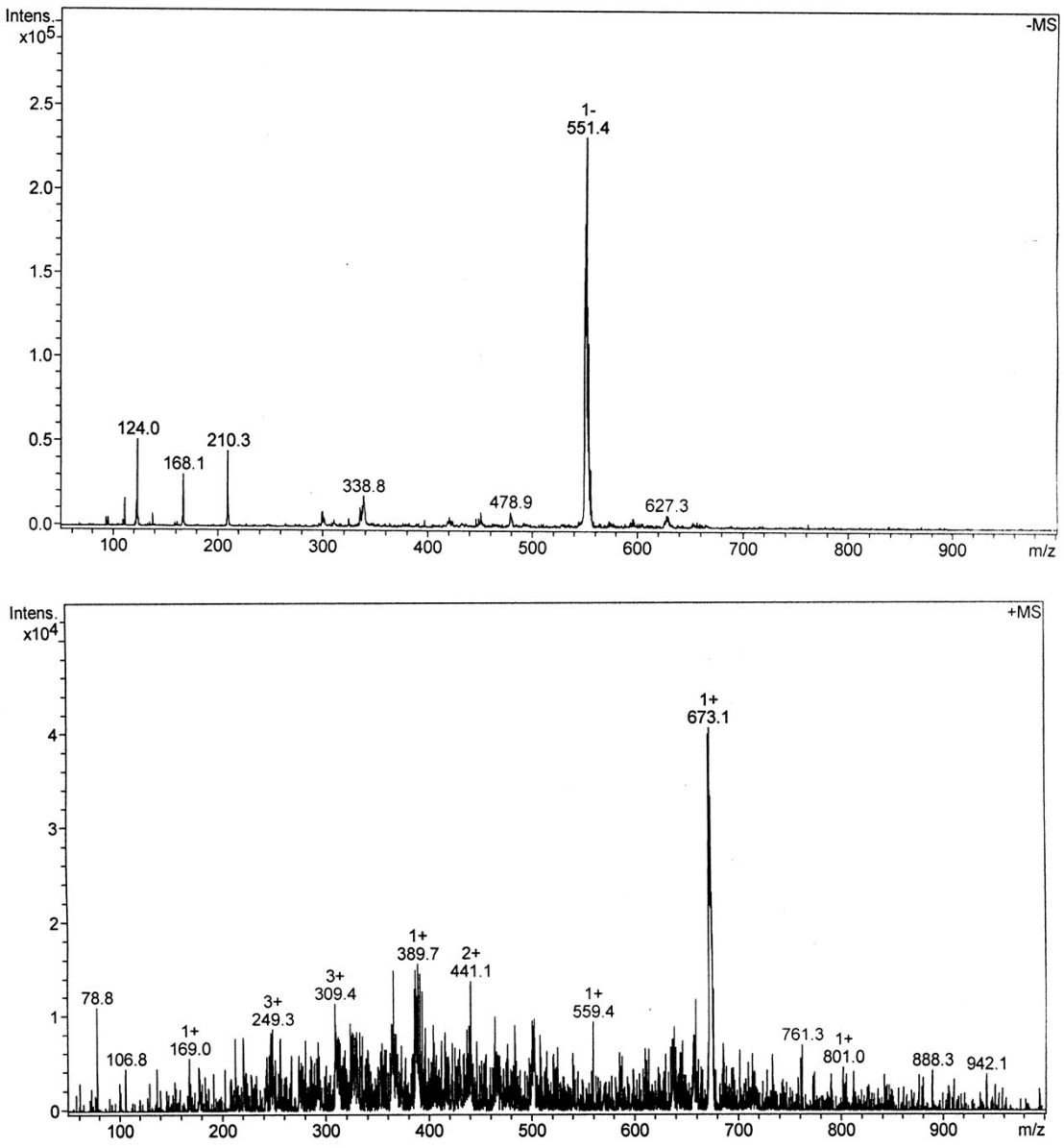

Fig. S4. The mass spectra of **Rut-Pt** in Tris-HCl buffer solution (containing 5% DMSO) for 0 h (top) and 48 h (down), respectively.

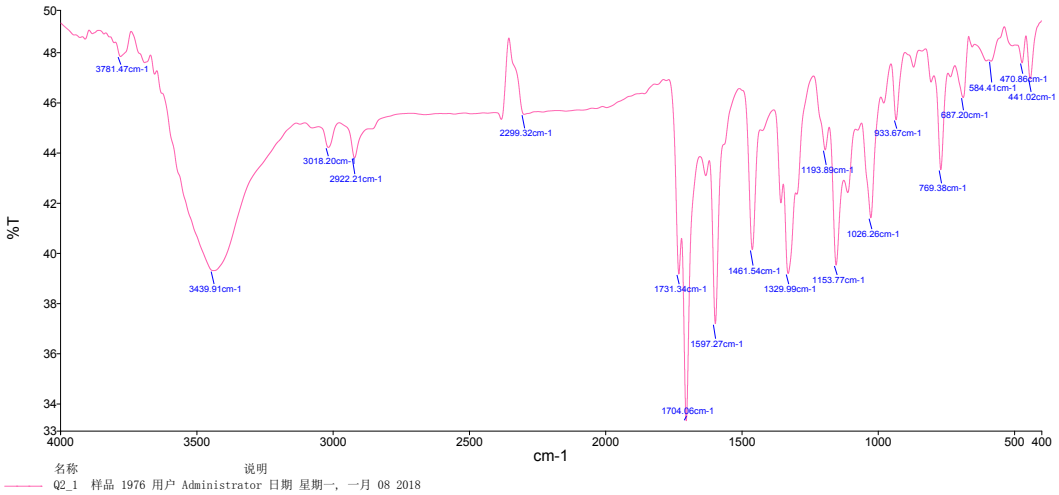

Fig. S5. IR (KBr) spectra of **Try-Pt**

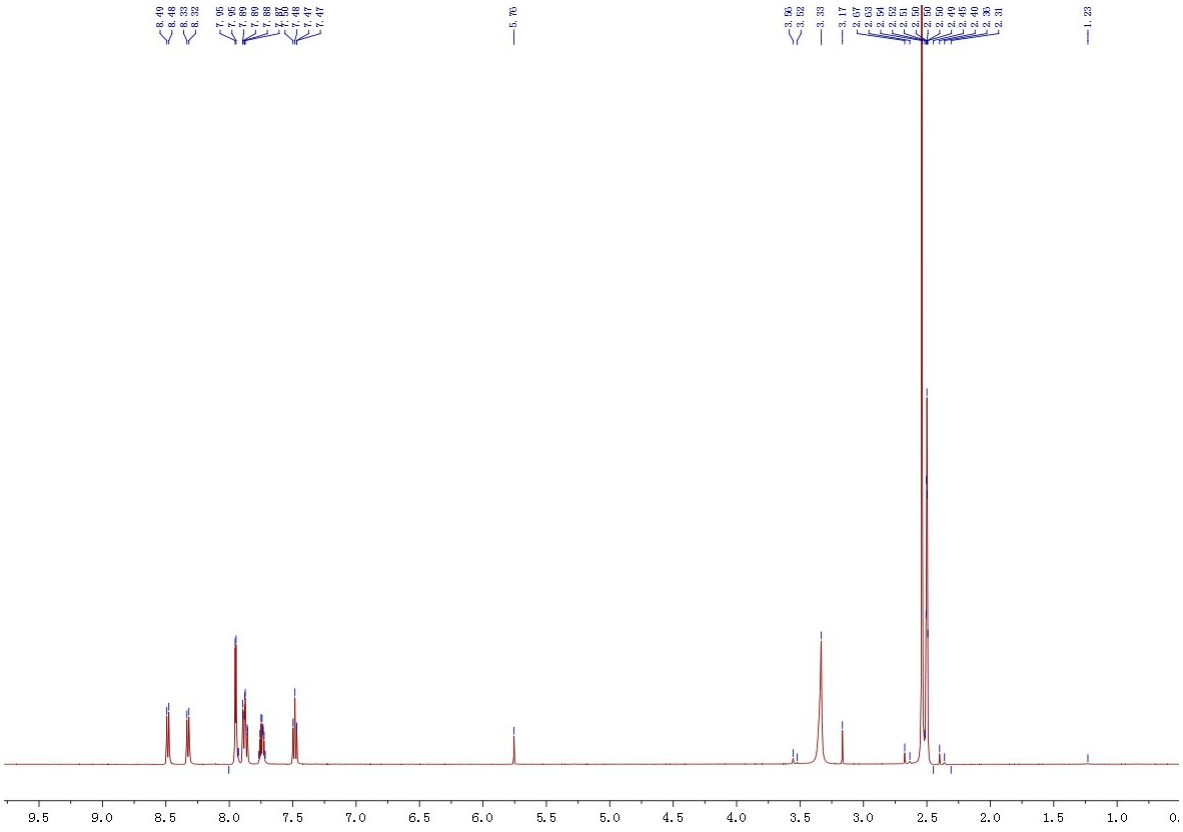

Fig. S6. ^{1}H NMR (500MHz, DMSO-d_6) for **Try-Pt**

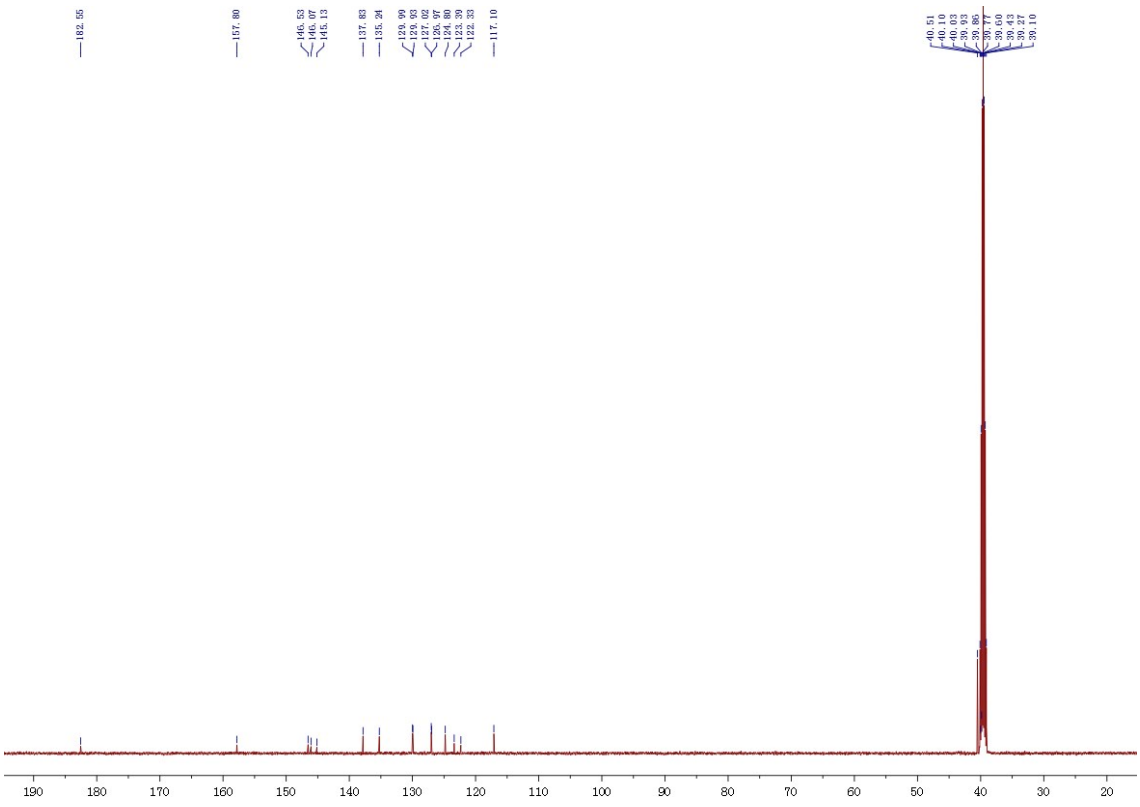

Fig. S7. ^{13}C NMR (126MHz, DMSO-d_6) for **Try-Pt**

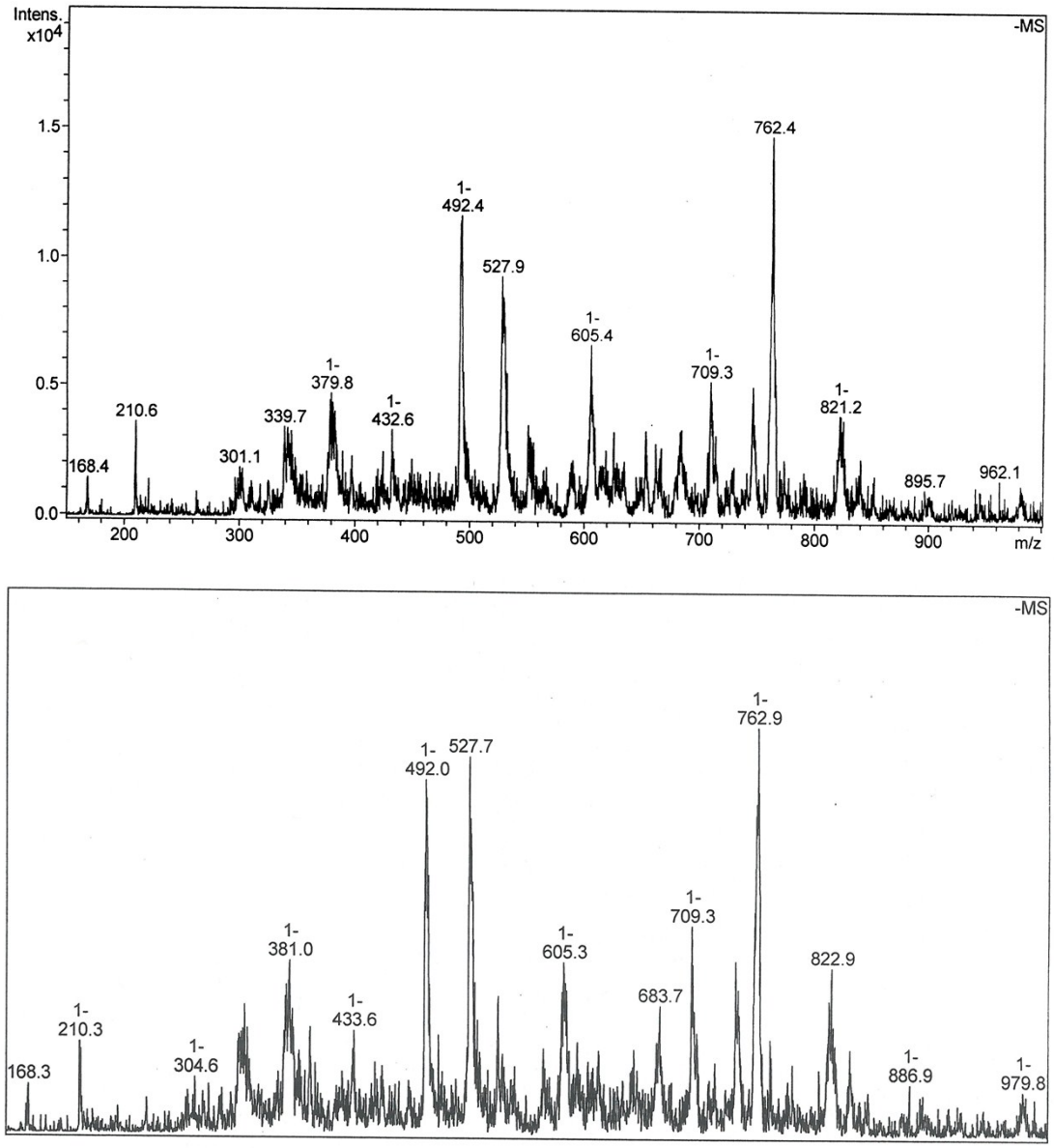

Fig. S8. The mass spectra of **Try-Pt** in Tris-HCl buffer solution (containing 5% DMSO) for 0 h (top) and 48 h (down), respectively.

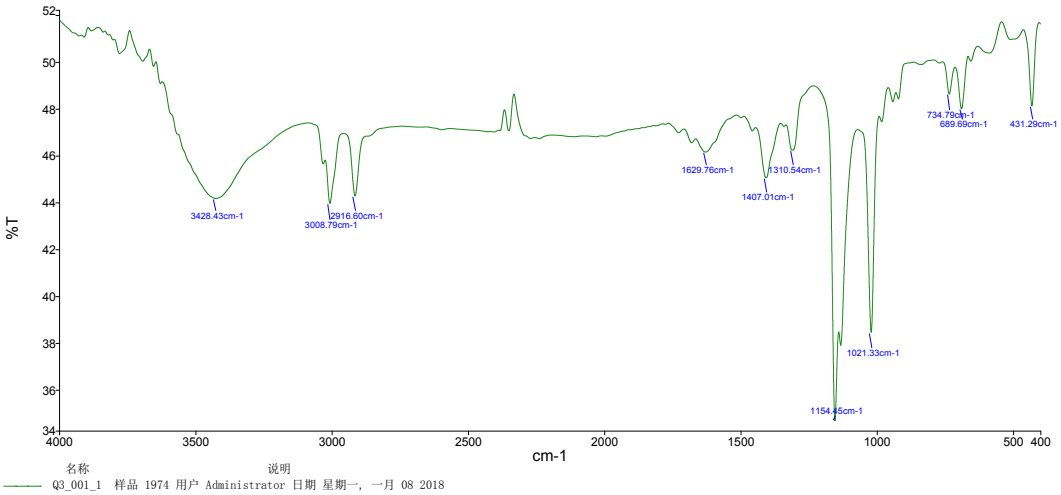

Fig. S9. IR (KBr) spectra of **ITry-Pt**

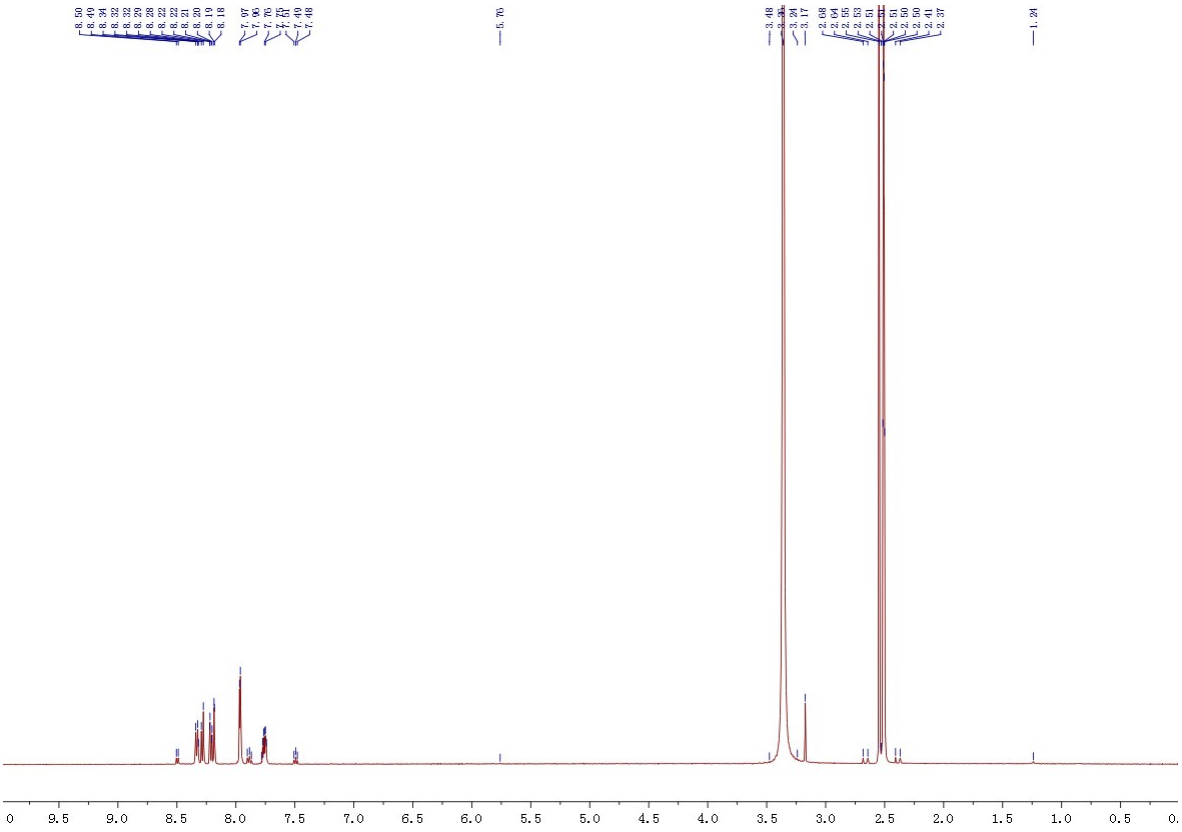

Fig. S10. ^{1}H NMR (500MHz, DMSO-d_6) for **ITry-Pt**

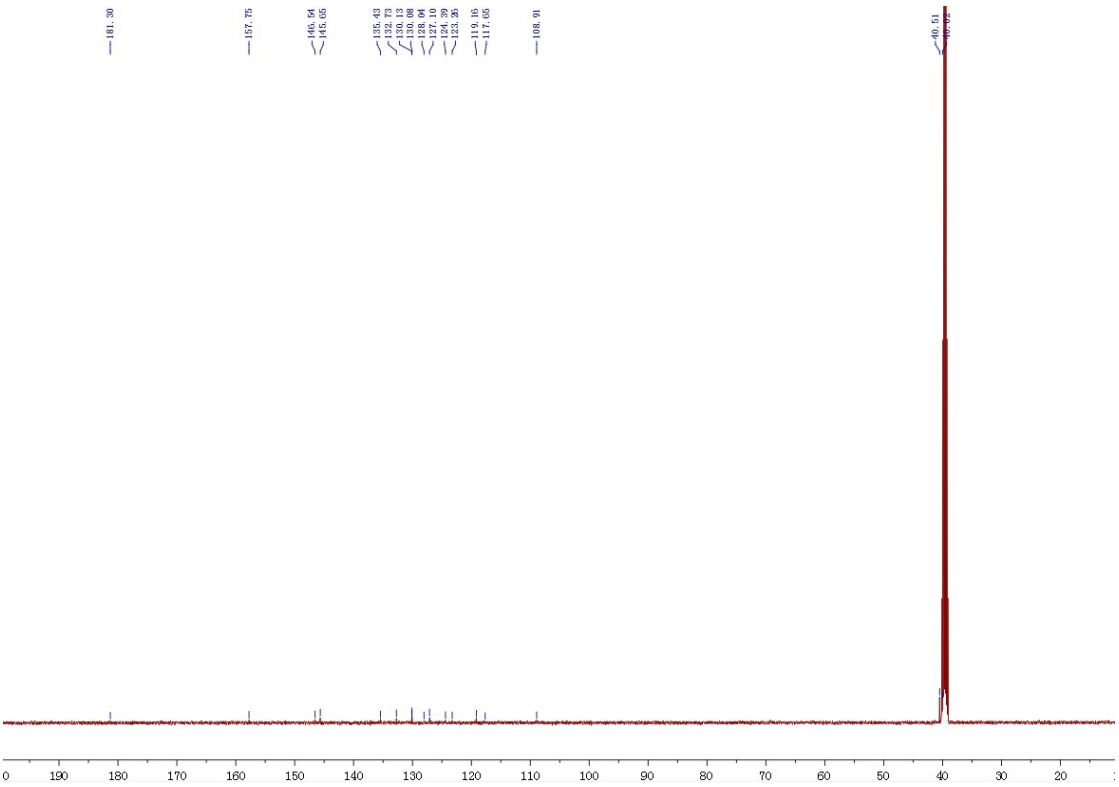

Fig. S11. ^{13}C NMR (500MHz, DMSO-d_6) for **ITry-Pt**

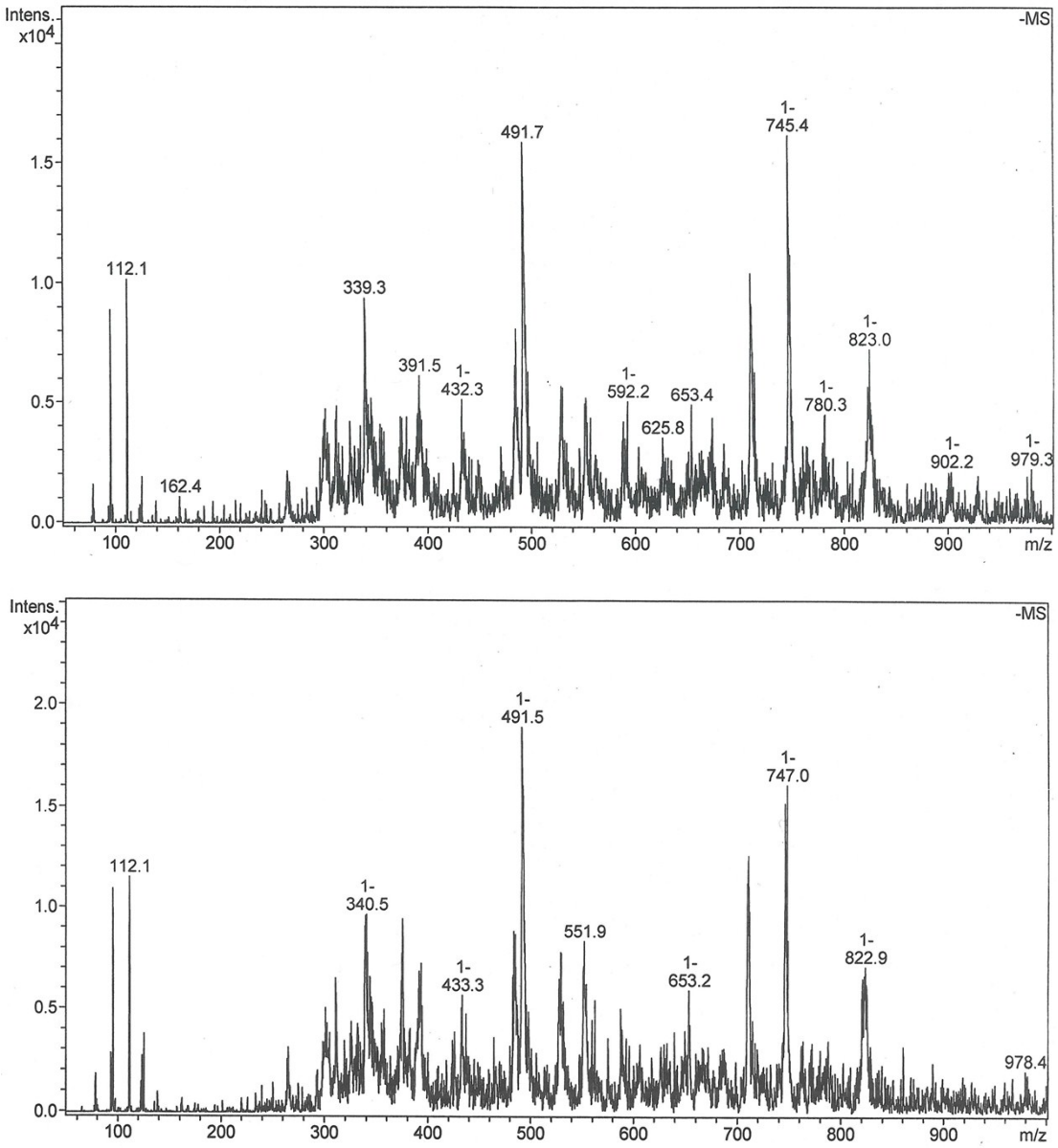

Fig. S12. The mass spectra of **ITry-Pt** in Tris-HCl buffer solution (containing 5% DMSO) for 0 h (top) and 48 h (down), respectively.

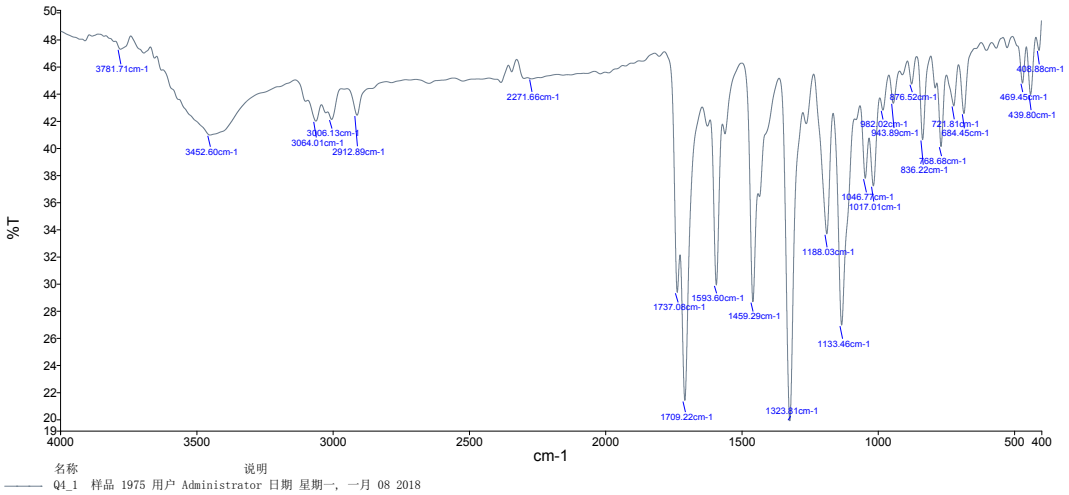

Fig. S13. IR (KBr) spectra of **BrTry-Pt**

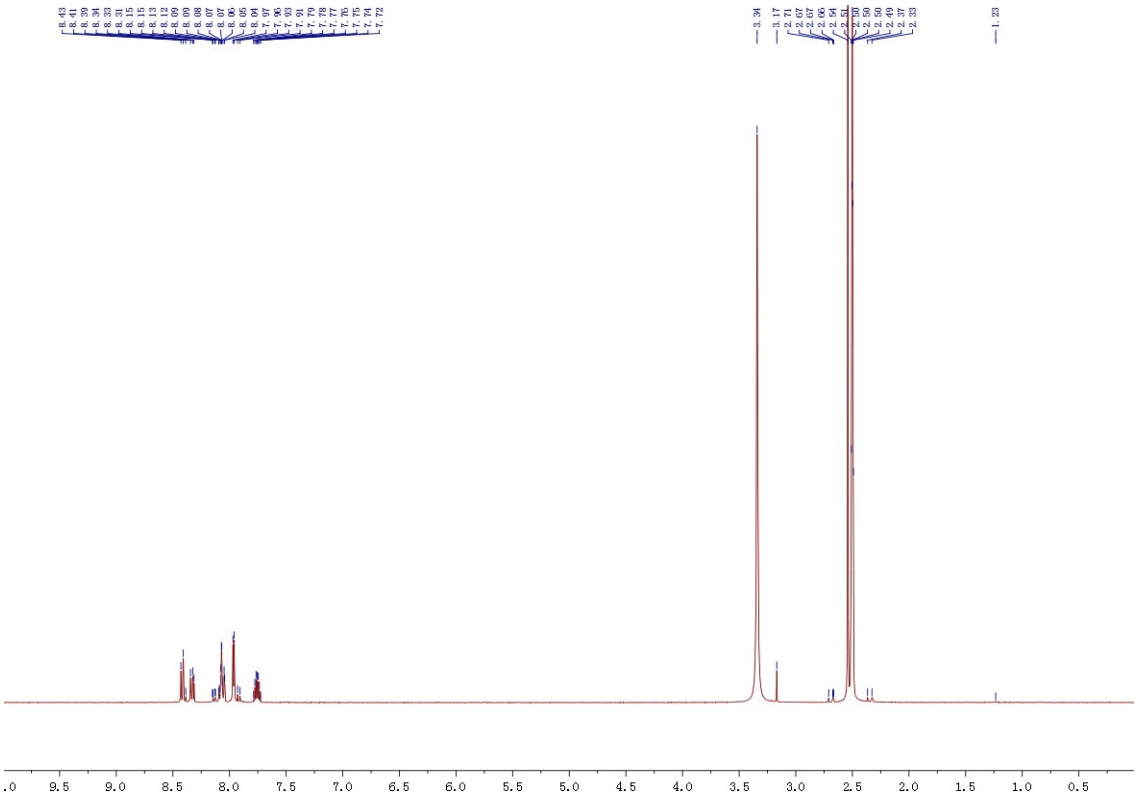

Fig. S14. ^{1}H NMR (500MHz, DMSO-d_6) for **BrTry-Pt**

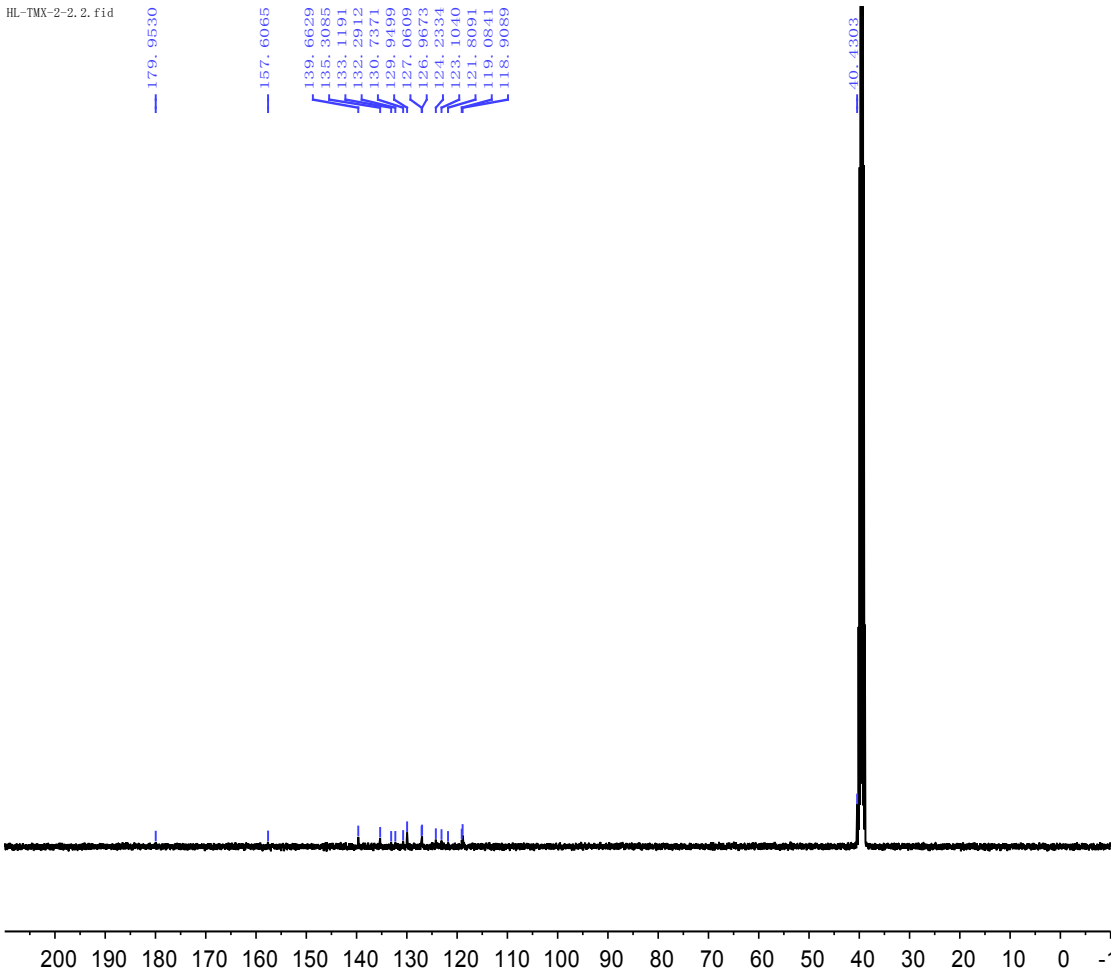

Fig. S15. ^{13}C NMR (500MHz, DMSO-d_6) for **BrTry-Pt**

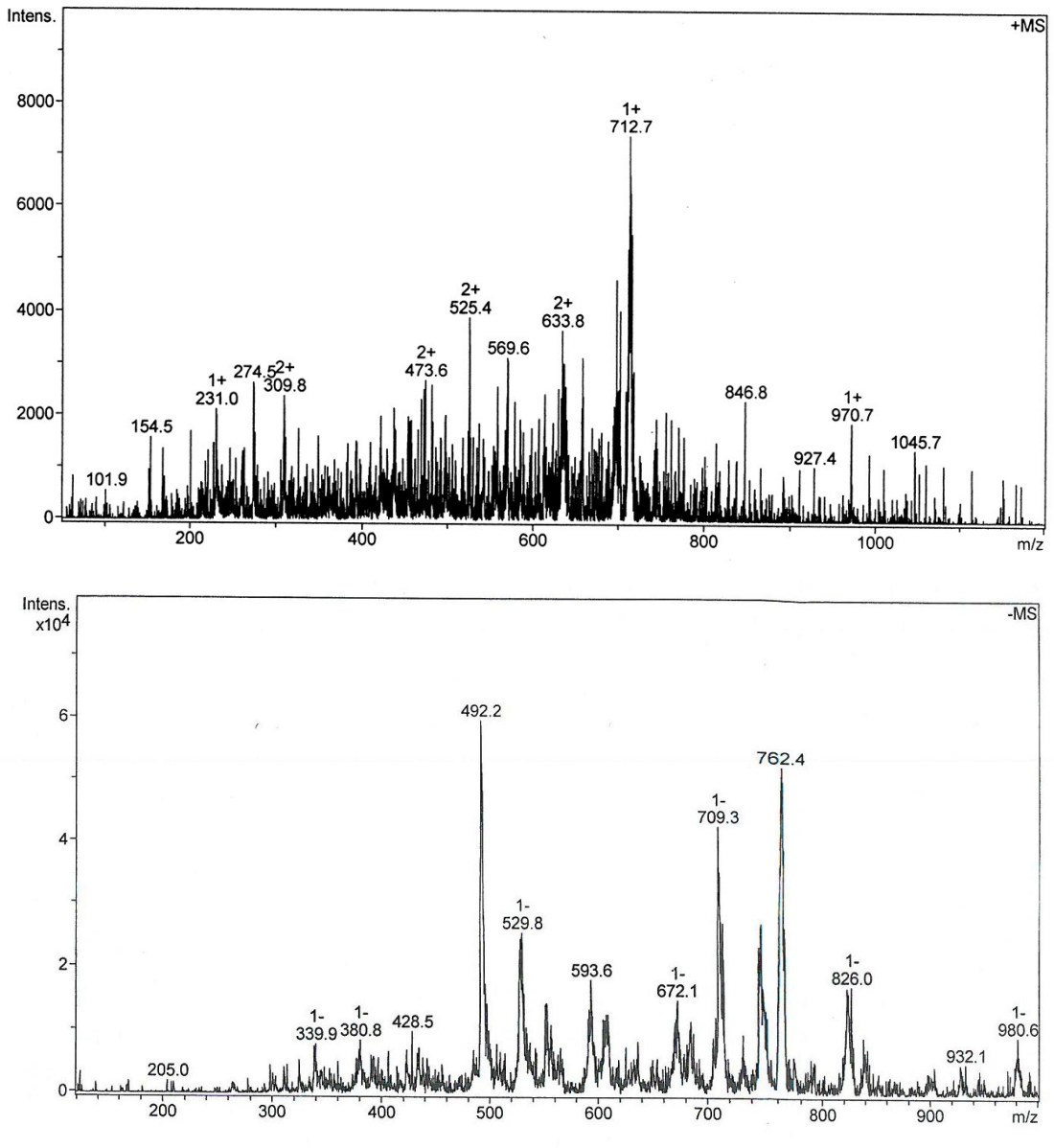

Fig. S16. The mass spectra of **BrTry-Pt** in Tris-HCl buffer solution (containing 5% DMSO) for 0 h (top) and 48 h (down), respectively.

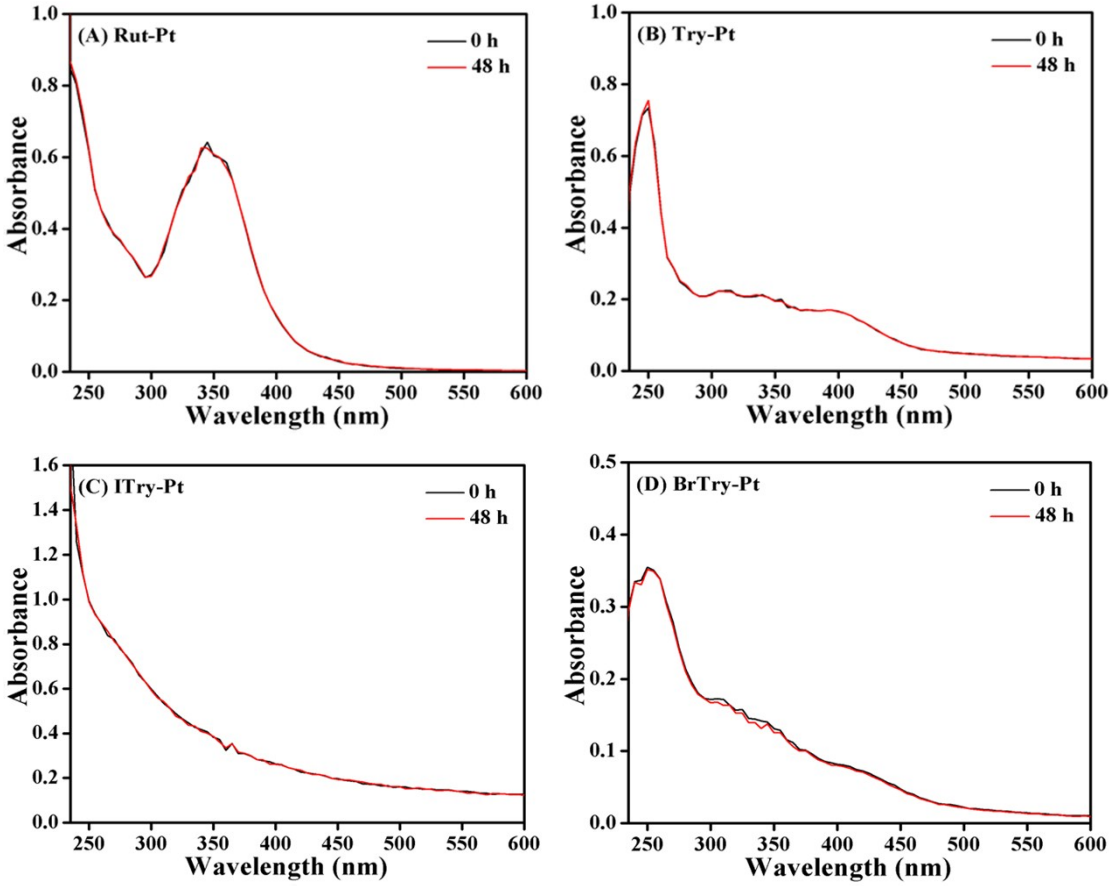

Fig. S17. UV-Vis absorption spectra of **Rut-Pt**, **Try-Pt**, **ITry-Pt** and **BrTry-Pt** (2.0×10^{-5} M) in TBS (Tris-HCl buffer solution, 10 mM, pH 7.35) solution in the time course 0 and 48 h, respectively.

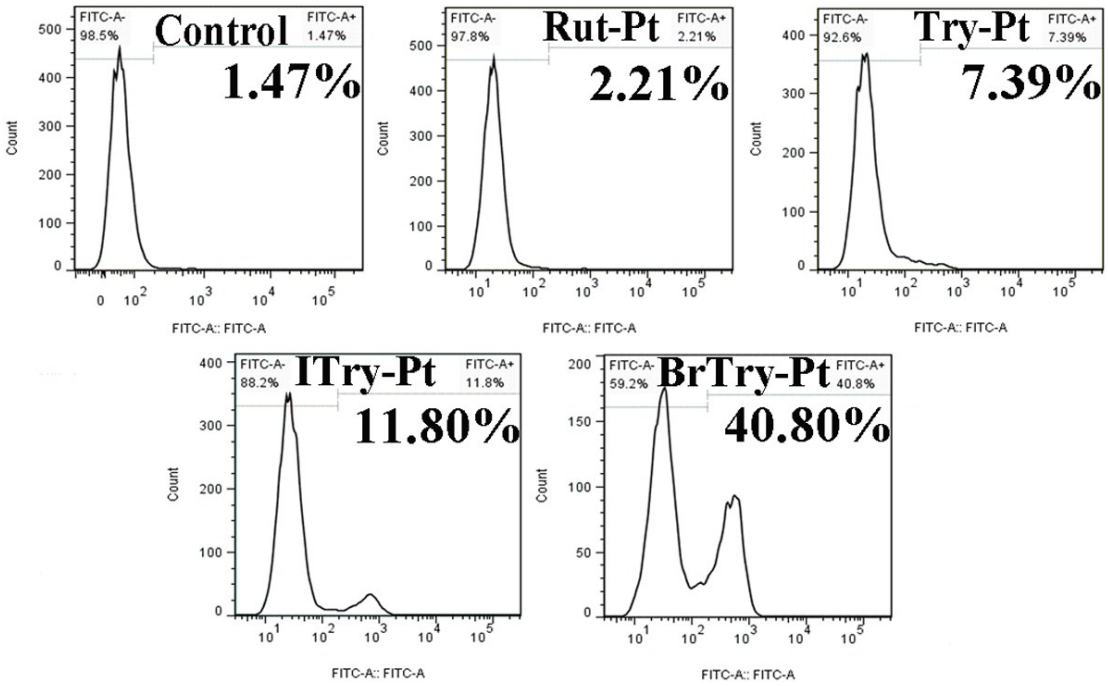

Fig. S18. Caspase-3 activation of T-24 cells in apoptosis induced by **Rut-Pt** (82 μM), **Try-Pt** (68 μM), **ITry-Pt** (19 μM) and **BrTry-Pt** (0.2 μM) for 24 h, respectively.

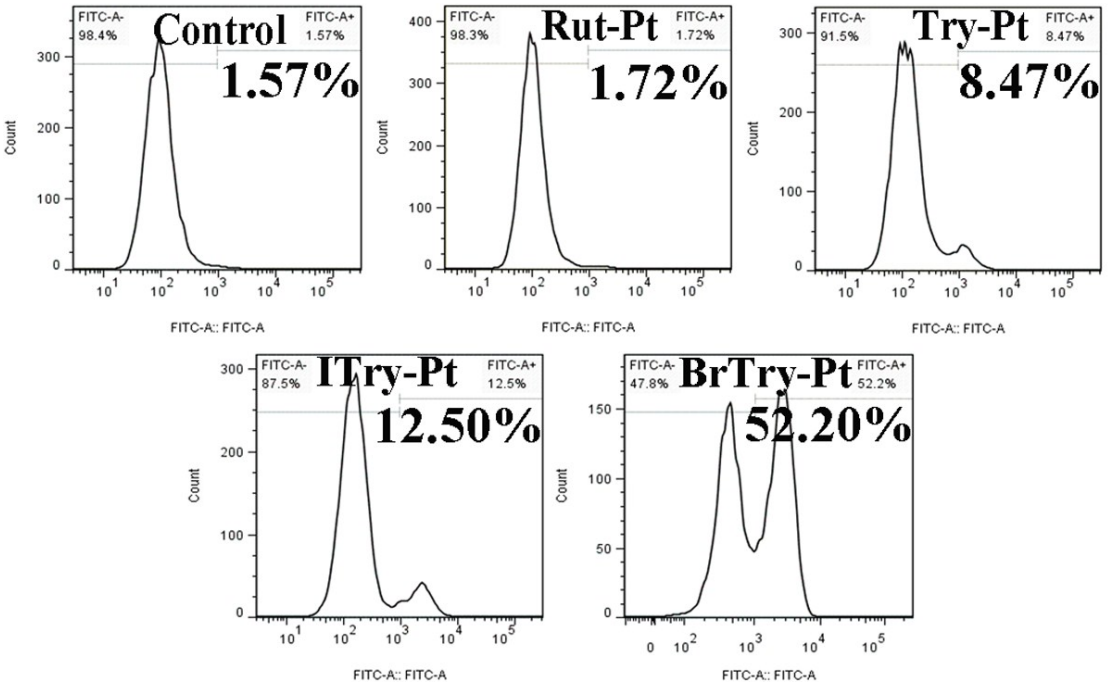

Fig. S19. Caspase-9 activation of T-24 cells in apoptosis induced by **Rut-Pt** (82 μM), **Try-Pt** (68 μM), **ITry-Pt** (19 μM) and **BrTry-Pt** (0.2 μM) for 24 h, respectively.

Table S14. Abbreviations in the study

TBS	Tris-HCl buffer
MTT	3-(4,5-dimethylthiazol-2-yl)-2,5-diphenyltetrazolium bromide
ROS	reactive oxygen species
IC_{50}	half maximal inhibitory concentration
T-24 cells	human bladder cancer cells
A549 cells	human carcinoma cells
Hep-G2 cells	human hepatocellular carcinoma cells
SK-OV-3 cells	human ovarian cancer cells
HeLa cells	human human sarcoma HeLa cancer cells
HL-7702 cells	human normal hepatocytes cells
PI	propidium iodide
$\Delta\psi$	mitochondrial membrane potential
JC-1	5,5′,6,6′-tetrachloro-1,1′,3,3′-tetraethylbenzimidazolylcarbocyanine

Experimental methods

Tris, RNase A, and propidium iodide (PI) were purchased from Sigma. The antibody was purchased from Abcam. The EGFP (enhanced green fluorescent protein) and c-myc gene vectors, the total RNA isolation kit and the two-step RT-PCR kit were purchased from TIANGEN. All the human cell lines were obtained from the Shanghai Institute for Biological Science (China). The abbreviations are listed in Table S14. Stock solutions of all the compounds (2.0 mM) were made in DMSO, and further dilutions to working concentrations were made with corresponding buffer.

Materials. Tris (EINECS No. 201-064-4, CAS Number: 77-86-1), RNase A (R6148), and propidium iodide (PI, CAS Number: 25535-16-4, EINECS No. 25535-16-4) were purchased from Sigma. The antibody of hTERT (Anti-Telomerase reverse transcriptase antibody, Y182, ab32020), c-myc (Anti-c-Myc antibody, Y69, ab32072), cyclin A (Anti-Cyclin A2 antibody, E23.1, ab38), CDK2 (Anti-Cdk2 antibody, E304, ab32147), cytochrome c (Anti-Cytochrome C antibody, 7H8.2C12, ab13575), bax (Anti-Bax antibody, E63, ab32503) and apaf-1 (Anti-APAF1 antibody, ab2001) were purchased from Abcam. The CaspGLOW^{TM} Fluorescein Active Caspase-3 Staining Kit (Catalog# K183-25, -100; Store kit at –20°C) and CaspGLOW^{TM} Fluorescein Active Caspase-9 Staining Kit (Catalog# K189-25, -100; Store kit at –20°C) were purchased from BioVision. FITC Annexin V Apoptosis Detection Kit I (BD556547) was purchased from Becton Dickinson bioscience (BD). Unless otherwise stated, spectroscopic titration experiments were carried out in 10 mM Tris-HCl (pH 7.35) containing 100 mM KCl. The total RNA isolation kit and the one-step RT-PCR kit (Quant One Step qRT-PCR Kit (Probe), FP304) were purchased from TIANGEN. All tumor cell lines (T-24, A549, Hep-G2, SK-OV-3, HeLa tumor cells and one normal HL-7702 cells) were obtained from the Shanghai Institute for Biological Science

(China). Stock solutions of all the compounds were made in DMSO, and further dilutions to working concentrations were made with corresponding buffer.

Instrumentation. Infrared spectra were obtained on a Perkine Elmer FT-IR Spectrometer. Elemental analyses (C, H, N) were carried out on a Perkin Elmer Series II CHNS/O 2400 elemental analyser. NMR spectra were recorded on a Bruker AV-500 NMR spectrometer. Fluorescence measurements were performed on a Shimadzu RF-5301/PC spectro fluorophotometer. ESI-MS spectra were obtained on Thermofisher Scientific Exactive LC-MS spectrometer (ThermalElctronic, USA). The circular dichroic spectra of DNA were obtained on a JASCO J-810 automatic recording spectropolarimeter operating at 25 °C. The region between 200 and 400 nm was scanned for each sample. MTT assay was performed on M1000 microplate reader (Tecan Trading Co. Ltd, Shanghai, China). Cell cycle and apoptosis analysis was recorded on FACS Aria II Flow Cytometer (BD Biocsiences, San Jose, USA). RT-PCR assay was performed on 7500fast RealTime PCR (ABI Co. Ltd., USA)

Cytotoxicity assay. The cell culture was maintained on RPMI-1640 medium supplemented with 10% fetal bovine serum, 100 U/mL penicillin and 100 μg/mL streptomycin in 25 cm^2 culture flasks at 37 °C humidified atmosphere with 5% CO_2. All cells to be tested in the following assays have a passage number of 3−6.

Cells 5.0×10^3 (T-24, A549, Hep-G2, SK-OV-3, HeLa tumor cells and one normal HL-7702 cells) per well were seeded in triplicate in 96-well plates and incubated for 24 h at 37 °C and 5% CO_2/95% air. Then graded amounts of compound were added to the wells in 10 μL of FBS free culture medium and the plates were incubated in a 5% CO_2 humidified atmosphere for 48 h. Six replica wells were used as controls. Cells were grew for 12 h before treatment to reach 70% confluency and 20 μL of tested various concentrations of compounds were added to each well. The final

concentration of the tested compounds were kept at 1.25, 2.5, 5, 10, 20, 40, 50, 60, 100, 150 μM, respectively. After 48 h of culture, 0.1 mg of MTT (in 20 μL of PBS) was added to each well, and cells were incubated at 37 °C for 6 h. The formed formazan crystals were then dissolved in 100 μL of DMSO and the absorbance was read by enzyme labeling instrument with 490/630 nm double wavelength measurement. The final IC_{50} values were calculated by the Bliss method (n = 5). All tests were repeated in at least three independent trials.

Cellular uptake of Pt(II) complexes. The T-24 tumor cells (~10 million cells) were treated with cisplatin (15 μM), **Rut-Pt** (82 μM), **Try-Pt** (68 μM), **ITry-Pt** (19 μM) and **BrTry-Pt** (0.2 μM) for 24 h at 37 °C in a humidified 5% CO_2 incubator. The spent media was removed, and the cells were washed with 5 mL of PBS, scraped, and collected in 5 mL of PBS. The scrapped cells were spun down, by centrifuging at 2500 rpm for 10 min. The cell pellet obtained was dissolved in 1 M NaOH (1 mL) and diluted with 2% (v/v) HNO_3 (5 mL) for determining whole cell cobalt content. Another set was treated similarly, nuclear fraction, nuclear proteins, membrane proteins and cytoplasmic protein were isolated as described by Schreiber et al [1], and the final solution was made up to 5 mL using 2% (v/v) HNO_3. The amount of cobalt taken up by the cells was determined by ICP-MS. The instrument was calibrated for Pt complexes using standard solutions containing 10, 50, 100, 500 and 1000 ppb Pt.

Apoptosis analysis. Apoptosis was detected by flow cytometric analysis of annexin V staining. Annexin V-FITC vs PI assay was performed as previously described [1-3]. Briefly, adherent T-24 cells were harvested and suspended in the annexin-binding buffer (5×10^5 cells/mL). Then, the T-24 cancer cells were incubated with annexin V-FITC and PI for 1 h at room temperature in the dark and immediately analyzed by flow cytometry. The data are presented as biparametric dot plots showing

PI red fluorescence vs annexin V-FITC green fluorescence.

Induction of ROS in T-24 cells. DCFH-DA is a freely permeable tracer specific for ROS. At the same time, DCFH-DA can be deacetylated by intracellular esterase to the non-fluorescent DCFH which is oxidized by ROS to the fluorescent compound 2',7'-dichloroflorescein (DCF, Beyotime Biotechnology, S0033). Therefore, the fluorescence intensity of DCF is proportional to the amount of ROS produced by the cells [4-6]. T-24 cells 1×10^6 were exposed to **Rut-Pt** (82 μM), **Try-Pt** (68 μM), **ITry-Pt** (19 μM) and **BrTry-Pt** (0.2 μM) for 24 h, respectively, and 1 mM H_2O_2 used as a positive control of ROS production. After the exposure, cells were harvested, washed once with ice-cold PBS and incubated with DCFH-DA (100 μM in a final concentration) at 37 ºC for 15 min in the dark [5,6]. Finally, the cells were washed again and maintained in 1 mL PBS. The ROS generation was assessed from 10,000 cells each sample by flow cytometric analysis with excitation and emission wavelengths of 488 and 530 nm, respectively.

Δψm loss. The loss of mitochondrial membrane potential (Δψ) was assessed using a lipophilic cationic fluorescent probe, JC-1 (5,5′,6,6′-tetrachloro-1,1′,3,3′-tetraethylbenzimidazolylcarbocyanine; Beyotime Biotechnology, C2006). SK-OV-3/DDP tumor cells treated with **Rut-Pt** (82 μM)**, Try-Pt** (68 μM), **ITry-Pt** (19 μM) and **BrTry-Pt** (0.2 μM) for 24 h were incubated with 5 μg/mL JC-1 for 30 min at 37 °C and examined under the fluorescence microscopy. The emission fluorescence for JC-1 was monitored at 530 and 590 nm, under the excitation wavelength at 488 nm. These cells were treated with **Rut-Pt** (82 μM), **Try-Pt** (68 μM), **ITry-Pt** (19 μM) and **BrTry-Pt** (0.2 μM) for 24 h and then analyzed by JC-1 flow cytometry. The orange-red emission of the dye is attributable to a potential-dependent aggregation in the

mitochondria, which reflects the Δψ. Green fluorescence reflects the monomeric form of JC-1, appearing in the cytosol after mitochondrial membrane depolarization.

Induction of Ca^{2+} fluctuation in T-24 cells. The level of intracellular free Ca^{2+} is decided by using a fluorescent dye Fluo-3 AM which can across the cell membrane and be cut into Fluo-3 by intracellular esterase (Beyotime Biotechnology, S1056). The Fluo-3 can specifically combine with the Ca^{2+} and has a strong fluorescence with an excitation wavelength of 488 nm. After exposed to **Rut-Pt** (82 μM), **Try-Pt** (68 μM), **ITry-Pt** (19 μM) and **BrTry-Pt** (0.2 μM) for 24 h, respectively, the T-24 tumor cells were harvested and washed twice with PBS, then resuspended in Fluo-3 AM (5.0 mM) for 30 min in dark. Detection of intracellular Ca^{2+} was carried by Flow cytometer at 525 nm excitation wavelength.

Telomerase Inhibition (TRAP Assay). The telomerase activity was assayed using a TRAP-silver staining assay kit (Sigma, #NKJ15DLM). The telomerase extract was prepared from the T-24 cells: a total of 5×10^6 T-24 tumor cells untreated or treated with **Rut-Pt** (82 μM), **Try-Pt** (68 μM), **ITry-Pt** (19 μM) and **BrTry-Pt** (0.2 μM) were pelleted, and the cells were washed with 5 mL of PBS, scraped and lysed for 30 min on ice. Finally, the lysate was centrifuged at 13 000 rpm for 30 min at 4 °C; the supernatant was collected and stored at −80 °C before use [6,7]. The TRAP assay was performed by following previously published procedures [7-9]. Telomerase extract was prepared from T-24 cells. A modified version of the TRAP assay was used [8]. PCR was performed in a final 50 mL reaction volume composed of reaction mix (45 mL) containing Tris-HCl (20 mM, pH 8.0), deoxynucleotide triphosphates (50 mM), $MgCl_2$ (1.5 mM), KCl (63 mM), EGTA (1 mM), Tween-20 (0.005%), BSA (20 mg/mL), primer H21T (3.5 pmol; 5'-$G_3[T_2AG_3]_3$-3'), primer TS (18 pmol; 5'-AATCCGTCGAGCAGAGTT-3'), primer Cxext (22.5 pmol; 5'-

GTGCCCTTACCCTTACCCTTACCCTAA-3'), primer NT (7.5 pmol; 5'-ATCGCTTCTCGGCCTTTT-3'), TSNT internal control (0.01 amol; 5'-ATTCCGTCGAGCAGAGTTAAAAGGCCGAGAAGCGAT-3'), Taq DNA polymerase (2.5 U), and telomerase (100 ng). Compounds or distilled water was added (5 mL). PCR was performed in an Eppendorf Master cycler equipped with a hot lid and incubated for 30 min at 30 ℃, followed by 92 ℃ 30 s, 52 ℃ 30 s, and 72℃ 30 s for 30 cycles. After amplification, loading buffer (8 mL; 5×TBE buffer, 0.2% bromophenol blue, and 0.2% xylene cyanol) was added to the reaction. An aliquot (15 mL) was loaded onto a nondenaturing acrylamide gel (16%; 19:1) in 1×TBE buffer and resolved at 200 V for 1 h. Gels were fixed and then stained with $AgNO_3$.

Determination of Caspase-3 and Caspase-9 Activity by Flow Cytometric Analysis. The measurement of caspase-3 and caspase-9 activity was performed by CaspGLOWTM Fluorescein Active Caspase-3 and Caspase-9 Staining Kit. 1×10^6 T-24 cells were cultured for 24 h. After a treatment with each compoud for 24 h, T-24 cells were harvested and washed 3 times with cold PBS and were then mixed with 300 μL culture. 1 μL of FITC-DEVD-FMK or FITC-LEHD-FMK was consequently added and incubated for 1.0 h at 37 °C incubator with 5% CO_2. The T-24 cells were then examined by a FACSAria II flow cytometer equipped with a 488 nm argon laser and results were represented as the percent change on the activity comparing with the untreated control. [1-13]

RNA extraction. The cell pellets harvested from each well of the culture plates were lysed in RZ Lysis solution. RNA was extracted with RNAsimple Total RNA kit (TIANGEN) according to manufacturer's protocol and eluted in distilled, deionized water with 0.1% diethyl pyrocarbonate (DEPC) to a final volume of 50 μL. RNA was stored at −80 °C before use.

RT-PCR. Total RNA was used as a template for reverse transcription using the following protocol: each 20 μL reaction contained 2.0 μL 10×RT mix., 2.0 μL dNTP (2.5 mM), 2.0 μL Oligo-dT15 primer, 1.0 μL Quant Reverse Transcriptase, 10 μL DEPC-H_2O, and 2 μg of total RNA. Briefly, RNA and oligo dT15 primer was incubated at 37 °C for 60 min and then immediately placed on ice. Finally, the reacted solution was stored at −80℃. Real-time PCR was performed on 7500 fast Real-Time PCR (ABI Co. Ltd, USA) by using 2.5×RealMasterMix/20×SYBR solution (TIANGEN), according to the manufacturer's protocol. The total volume of 20 μL real-time RT-PCR reaction mixtures contained 9.0 μL of 2.5×RealMasterMix/20×SYBR solution, 0.25 μM each of forward and reverse primers, 1.0 μL of cDNA, and nuclease-free water. The program used for all genes consisted of a denaturing cycle of 3 min at 95 °C, 45 cycles of PCR (95 °C for 20 s, 58 °C for 30 s, and 68 °C for 30 s), a melting cycle consisting of 95 °C for 15 s, 65 °C for 15 s, and a step cycle starting at 65 °C with a 0.2 °C/s transition rate to 95 °C. The specificity of the real-time RT-PCR product was confirmed by melting curve analysis. The PCR product sizes were confirmed by agarose gel electrophoresis and ethidium bromide staining. Three replications were performed, and then hTERT and c-myc mRNA levels were normalized with the GAPDH mRNA level of each sample. Results of real-time PCR were analyzed using the $2^{-\Delta\Delta CT}$ method in the program Origin 8.0 to compare the transcriptional levels of hTERT and c-myc genes in each sample relative to nondrug treated control.

Western blotting. The T-24 tumor cells harvested from each well of the culture plates were lysed in 150 μL of extraction buffer consisting of 149 μL of RIPA Lysis Buffer and 1 μL PMSF (100 mM). The suspension was centrifuged at 10000 rpm at 4 °C for 10 min, and the supernatant (10 μL for each sample) was loaded onto 10%

polyacrylamide gel and then transferred to a microporous polyvinylidene difluoride (PVDF) membrane. Western blotting was performed using anti-c-myc, hTERT, cytochrome c, bcl-2, capase-3, bax, apaf-1, caspase-9 and β-actin antibody and horseradish peroxidase-conjugated antimouse or antirabbit secondary antibody. Protein bands were visualized using chemiluminescence substrate.

Transfection. After the T-24 tumor cells (8.0×10^5) were grew in 3 cm Petri dishes for 24 h, DNA transfections were performed using the following procedure. Firstly, 2.0 μg EGFP plasmid (addgene, Plasmid #16601) [10] and 2.0 μg c-myc plasmid (addgene, Plasmid #15949) [11,12] were cotranfected into T-24 cancer cells using Lipo2000 (Invitrogen). Then, **Rut-Pt** (82 μM), **Try-Pt** (68 μM), **ITry-Pt** (19 μM) and **BrTry-Pt** (0.2 μM) were added into medium, respectively, after 6 h of transfection. After another 24 h of drug treatment, the cells were imaged using Nikon TE2000 (Japan) scanning fluorescence microscope and studied by Luciferase Reporter Gene Assay Kit.

Statistical analysis. The experiments have been repeated from three to five times, and the results obtained were presented as means±standard deviation (SD). Significant changes were assessed by using Student's *t* test for unpaired data, and p values of <0.05 were considered statistically significant.

References

1 E. Schreiber, P. Matthias, M. M. Mueller and W. Schaffner, Nucleic Acids Res., 1989, **17**, 6419.

2 L. Chong, B. van Steensel, D. Broccoli, H. Erdjument-Bromage, J. Hanish, P. Tempst and T. de Lange, Science, 1995, **270**, 1663–1667.

3 D. Broccoli, A. Smogorzewska, L. Chong and T. de Lange, Nat. Genet., 1997, **17**, 231–235.

4 S. Lin, M. Fujii and D. X. Hou, Arch. Biochem. Biophys., 2003, **418**, 99–107.

5 R. M. Sainz, J. C. Mayo, D. X. Tan, S. Lopez-Burillo, M. Natarajan and R. J. Reiter, Res. Commun., 2003, **302**, 625–634.

6 Z.-F. Chen, Q.-P. Qin, J.-L. Qin, Y.-C. Liu, K.-B. Huang, Y.-L. Li, T. Meng, G.-H. Zhang, Y. Peng, X;-J. Luo and H. Liang, J. Med. Chem., 2015, **58**, 2159–2179.

7 A. De Cian, G. Cristofari, P. Reichenbach, E. De Lemos, D. Monchaud, M.-P. Teulade-Fichou, K. Shin-ya, L. Lacroix, J. Lingner and J.-L. Mergny, PNAS, 2007, **104**, 17347–17352.

8 J. E. Reed, A. A. Arnal, S. Neidle, R. Vilar, J. Am. Chem. Soc., 2006, **128**, 5592–5993.

9 G. Krupp, K. Kühne, S. Tamm, W. Klapper, K. Heidorn, A. Rott and R. Parwaresch, Nucleic Acids Res., 1997, **25**, 919–921.

10 M. Chalfie, Y. Tu, G. Euskirchen, W. W. Ward and D. C. Prasher, Science, 1994, **263**, 802–805.

11 T.-C. He, A. B. Sparks, C. Rago, H. Hermeking, L. Zawel, L. T. da Costa, P. J. Morin, B. Vogelstein and K. W. Kinzler, Science, 1998, **281**, 1509–1512.

12 Q.-P. Qin, T. Meng, M.-X. Tan, Y.-C. Liu, X.-J. Luo, B.-Q. Zou and H. Liang, Eur. J. Med. Chem., 2018, **143**, 1387–1395.

13 T. Meng, S.-F. Tang, Q.-P. Qin, Y.-L. Liang, C.-X. Wu , C.-Y. Wang, H.-T. Yan, J.-X. Dong and Y.-C. Liu, Med. Chem. Commun., 2016, **7**, 1802–1811.